Extracellular vesicles promote migration despite vemurafenib treatment in malignant melanoma cells

Afrodité Németh
Pázmány Péter Catholic University
Gréta L. Bányai
Pázmány Péter Catholic University
Nikolett K. Dobos
Pázmány Péter Catholic University
Tamás Kós
Pázmány Péter Catholic University
Anikó Gaál
Research Centre for Natural Sciences
Zoltán Varga
Research Centre for Natural Sciences
Edit I. Buzás
Semmelweis University
Delaram Khamari
Semmelweis University
Magdolna Dank
Semmelweis University
István Takács
Semmelweis University
A. Marcell Szász
Semmelweis University
Tamás Garay (garay.tamas@itk.ppke.hu)
Pázmány Péter Catholic University

Research Article

Keywords: Extracellular vesicles, melanoma, vemurafenib, single cell tracking, cell migration

Posted Date: August 21st, 2023

DOI: https://doi.org/10.21203/rs.3.rs-3262957/v1

Abstract

Extracellular vesicles (EVs) were found to be one group of the determining factors in intercellular communication and have been shown to have a crucial role in metastasis formation and drug resistance. Malignant melanoma (MM) is one of the deadliest forms of skin cancers, because of its high metastatic potential and often acquired resistance to oncotherapies. BRAF mutation is the most prevalent genetic aberration in MM, which implicates BRAF (e.g. vemurafenib) or combined BRAF/MEK inhibitor therapy. Herein, we analyzed the role of EVs in MM progression and investigated if EVs can maintain their role in metastasis promotion during vemurafenib treatment.

Five pairs of syngeneic melanoma cell lines were treated with EVs isolated from their or their pair's supernatant. EVs' impact on melanoma cells' proliferation was investigated using cell viability and spheroid growth assays. Furthermore, to investigate changes in cell migration, mean squared displacement (MSD) and total travelled distance (TTD) were calculated based on video microscopy measurements and single cell tracking.

In most of the cases, EV treatments did not affect cell proliferation and spheroid growth, however, their migration-promoting role was more prominent. Additionally, EVs originating from more resistant cells could counteract the inhibitory effect of vemurafenib.

In conclusion, our findings provide further details to understand the complex role of EVs in tumor promotion, progression and single-agent vemurafenib resistance in MM.

1. Introduction

Extracellular vesicles (EVs) are small lipid-bound particles loaded and decorated with different types of macromolecules and can be found in all body fluids. These particles are important contributors to both local and systematic communications, there-fore several studies suggest that EVs may serve as prognostic and predictive biomarkers [1]. Elevated plasma EV level correlated with inferior prognosis in non-small cell lung [2], colon [3], head and neck [4] cancer or melanoma [5]. Of note, in oral squamous cell carcinoma patients the plasma EV level was decreased after the tumor mass has been reduced surgically [6]. In addition, elevated level of plasma EV-associated protein was accompanied by brain metastasis [7]. In line with clinical observations, highly metastatic melanoma-derived EVs supported metastasis formation and tumor dissemination in mice [5]. Thus, EVs are considered to play a determining role in the process of metastasis formation [8], [9].

EVs can play crucial roles in several steps of cancer progression. EVs can influence the tumor microenvironment by activating normal human fibroblasts [10] or inactivating macrophages and reprograming the secretory profile of monocytes [11]. Furthermore, melanoma cells-derived exosomes increase melanoma cell proliferation and inhibit their apoptosis [12]. Similarly, EVs can influence the recipient cells' metastatic potential, they can modulate migratory capacity [13], invasiveness [14], anchorage-independent cell growth [15] and pre-metastatic niche formation [16]. Moreover, cells with different

degrees of malignancy produce variable EV populations [17] and EVs from metastatic tumor-derived cell lines can increase the metastatic potential of less aggressive cell lines [18].

Metastasis formation is the primary cause of cancer-related deaths [19], thus due to their effect on metastasis formation, EVs could have a striking role in managing metastatic malignancies. One of the most metastatic tumors is melanoma [20], [21] with a 5-year survival of over 90% in patients with a localized tumor and only 16% in metastatic cases [22]. However, mutational analysis for BRAF or multigene testing of the primary lesion is not recommended for patients with cutaneous melanoma unless required to guide adjuvant or other systemic therapy or consideration of clinical trials, approximately 40–60% of melanoma cases harbor V600E mutation in BRAF, which leads to a constitutive mitogen-activated protein kinase (MAPK) signaling pathway activation [23]–[25]. In clinics, one of the potent BRAF inhibitors is vemurafenib [26]–[29].

In preclinical experiments, vemurafenib increases cell death [30], [31], decreases proliferation [32], [33] and also affects cell migration [34]–[36]. Furthermore, exposure to vemurafenib can also modify the released EVs' content [37], [38]. Unfortunately, after the first sensitive period, relapse, and resistance to vemurafenib are observed in most melanoma cases [39]. Several mechanisms, such as genetic, epigenetic and/or transcriptomic changes, or changes in EV trafficking can lead to vemurafenib re-sistance [40]–[42]. In addition, emerging vemurafenib resistance is accompanied by increased metastasis formation [43], [44].

Accordingly, our aim was to investigate the role of EVs in cancer progression us-ing in vitro melanoma models of syngeneic pairs of cell lines. In each of the used five pairs of cell lines, one cell line modelled an earlier, less advanced stage of the tumor (e.g. originating from a primary site tumor or isolated from a tumor specimen taken before the start of vemurafenib therapy). In contrast, the other cell line represented a more advanced stage of the disease (e.g. isolated after relapse, isolated from a meta-static site or selected as the most tumorigenic sub-clone in mice). EVs produced by the cell lines were characterized, and their effects on proliferation and migration were investigated in vitro. In parallel, our aim was also to evaluate whether vemurafenib could attenuate the possible effects of EV treatment. In order to understand underlying biological processes, we administered vemurafenib as a single agent to our cell cultures.

2. Materials and Methods

2.1 Cell lines and culturing:

Melanoma cells used for the experiments were pairwise originating from the same patient (i.e. representing the same genetic background) and modelling the less and more advanced stages of the given tumor.

Mel Pt-1, Mel Pt-3, Mel Pt-4 pair of cell lines were established and kindly provided by Professor Peter Hersey from the Oncology and Immunology Unit, Calvary Mater Newcastle Hospital and the Kolling

Institute, Royal North Shore Hospital, University of Sydney, NSW, Australia [45]. The cell line pairs “pre” members were isolated before vemurafenib treatment and “post” members during vemurafenib treatment, each patient was partially responsive to vemurafenib and all cell lines are harboring BRAF V600E mutations [45]. The BRAF V600E mutant WM983A and WM983B cell lines are available at Wistar Institute, Philadelphia, PA, USA, and the A2058 cell line harboring a BRAF V600E mutation at ATCC. M1 cell line was established from A2058 cells as the sub-clone with the greatest tumorigenic potential in immunosuppressed mice [46].

All cells were cultured in DMEM (4.5g/L glucose with L-glutamine and Sodium Pyruvate, Capricorn-Scientific) supplemented with 10% fetal bovine serum (FBS, EuroClone) and 1% penicillin-streptomycin-amphotericin (Lonza) at 37°C in 5% CO2 atmosphere.

2.2. Isolation of EVs from cell-culture supernatant:

Prior to harvest the supernatant, cells were grown in all cases in three 75 cm2 tissue culture flasks until 50–60% confluency, then cells were washed 2 times with PBS (Capricorn-Scientific) and cultured in DMEM supplemented with 1% EV-depleted FBS (Biowest) for three days. The collected supernatants were centrifuged at 500 g for 5 minutes to remove floating cells and cell debris. Supernatants were stored at -80°C until further use. On the day of the experiments, the frozen supernatants were thawed slowly, centrifuged at 3,000 g for 15 minutes, and filtered through a 0.2 µm syringe filter unit (Sarstedt). Then the filtered samples were subjected to ultracentrifugation (Beckman L7-55 Ultracentrifuge, TYPE 50.2 Ti rotor) at 100,000 g for 1.5 hours at 4°C and the pellets (EV) were suspended in 300 µl of PBS and used for treatments on the day of the isolation.

2.3. Characterization of EVs:

EV samples were first verified using Dynamic Light Scattering (DLS). The isolation was considered successful if the EV sample’s main particle population size was in the range of cell-culture supernatant EVs [47] and the supernatant didn’t contain particles larger than 10 nm. Total protein concentration was quantified by Qubit® Protein Assay Kit (Thermo Fisher Scientific) according to the manufacturer’s instructions, and lipid concentration was determined by sulfophosphovanillin lipid assay [48]. Particle concentration and size distribution were evaluated by Nano Particle Tracking Analysis with ZetaView PMX120 NTA instrument (Particle Metrix GmbH, Inning am Am-mersee, Germany). EVs were characterized by flow cytometry (FCM) with a CytoFlex flow cytometer (Beckman Coulter Inc., Brea, California, USA) using commonly used membrane markers. Briefly, the isolated EVs were first attached to 3 µm aldehyde/sulfate latex beads (4% w/v; Thermo Fisher Scientific). The samples were incubated with 1,000-fold diluted latex beads (in PBS) at a 1:1 ratio for 30 minutes at room temperature (RT), 320 rpm on a thermo-shaker. The bead concentration was chosen to be at least 300 EV per latex particle. Then the latex beads were blocked with glycine (100 mM final concentration; Sigma-Aldrich) and BSA (1% final concentration; Sig-ma-Aldrich) for one hour at RT, 320 rpm. Blocking agents were removed by centrifugation at 3,000 g for 5 minutes, and the pellet was resuspended in PBS (latex beads volume was diluted 5 times). To fluorescently label EVs on the surface of the beads, the samples were stained using

Annexin V-FITC (1:1000; InvitrogenTM BMS500FI-100); and EpCAM (EGP40/1372; GeneTex GTX34694), CD81 (1D6; GeneTex GTX75436), CD63 (MEM-259; GeneTex GTX28219), CD9 (MEM-61; GeneTex GTX22215) as primary antibodies (1:100) and Alexa FluorTM 488-conjugated secondary antibody (1:200; Alexa FluorTM 488 goat anti-mouse IgG; Invitrogen A11029) for 30 minutes at 37°C, 320 rpm. Negative control was prepared by blocking the latex beads with glycine and BSA and incubating them with Annexin V-FITC and the secondary antibody. The samples were measured directly with the FCM instrument, and gating of the main latex population (in diameter of 3 µm) was performed with the CytExpert algorithm. All data is submitted to the EV-TRACK knowledgebase (EV-TRACK ID: EV230027) [49].

2.4. Cell viability (SRB) assays:

Vemurafenib (PLX4032, WVR) GI50 values for each cell line were determined by Sulforhodamine B (SRB) cell viability assays. Cells were seeded in a 96-well plate and after overnight attachment, treated with vemurafenib, EVs (10 µg/ml protein concentration) or both in DMEM supplemented with 10% EV-depleted FBS for 72 hours. Cells were fixed with 10% trichloroacetic acid and stained with SRB. After 15 minutes the stain was discarded, and the cells were washed with 1% acetic acid solution and dried out. The stain was dissolved in 10 mM Tris-HCl, pH 8 and absorbance was determined at 570 nm.

2.5. Spheroid formation assay:

To create spheroid cultures, cells were seeded in previously coated U-bottom 96 well plates. For coating the wells, 30 µl of 25 mg/ml poly(2-hydroxyethyl methacrylate) (poly HEMA, Merck) dissolved in 96% ethanol solution was added in each well, and plates were put on a rocking platform until the complete evaporation of the solution (3 days). Cells were seeded at 1,000 cells/well density and kept in DMEM supplemented with 10% EV-depleted FBS and 0.04 mg/ml collagen (Merck). After seeding, the plates were centrifuged at 2,200 rpm for 10 minutes. After 24h incubation, EV treatment was performed using a final protein concentration of 10 µg/ml. To document spheroid growth, black and white pictures were taken daily for 7 days and evaluated using ImageJ. Spheroid size was quantified by calculating the signal intensity (CI) (i.e. darkness) of the spheroids considering spheroid area, integrated density (ID), and the median pixel intensity of the respective well using the following formula:

$$CI = 255 \times area - ID - (255 - median) \times area$$

2.6. Cell migration analysis by single-cell tracking:

Video-microscopy measurements were used to evaluate cell migration. Plates were prepared and treated as for SRB assays. Vemurafenib was applied in the following concentration: Mel Pt-1 pre/post, Mel Pt-4 pre/post: 10 µM, Mel Pt-3 pre 0.75 µM, Mel Pt-3 post 7.5 µM, WM983A: 0.05 µM, WM983B: 0.25 µM, A2058 and M1: 2.5 µM. After treatment, plates were placed into an inverted phase contrast microscope with an automatic stage and surrounding incubator (Nikon TIE microscope, Prior stage, Oko-Lab incubator) and kept at 37°C in 5% CO2 atmosphere. Time-lapse recording was performed for 24 hours with 10 minutes per frame rate. After pre-processing the images, single-cell tracking and determination of the XY coordinates of the cells were performed with the semiautomatic tracking tool CellTracker [50].

From the cells' coordinates, two different migration parameters were calculated: total travelled distance (TTD) and mean square displacement (MSD). TTD is calculated as the sum of the distance travelled by the cell between two consecutive images. MSD measures the average square displacement over increasing time intervals between two points [51]. To evaluate the effects of the treatments, first, both MSD and TTD values were averaged for control cells as a function of time. For the averaged-control and for each cell individually, area under the curve (AUC) was computed using MATLAB built-in function trapz() and ΔAUC were calculated as the difference between each individual cells' AUC and the averaged-control AUC, and ΔAUC values were averaged for each treatment group.

2.7. Statistical analysis:

Statistical differences between groups were determined using Kruskal-Wallis and Dunn's multiple comparison test, and a p-value less than 0.05 was considered as statistically significant. For results not enabling more specific statistical testing, data are shown as average ± 95% confidence interval in line with the $p < 0.05$ burden for statistical significance. GraphPad Prism 8 (GraphPad Software Inc., San Diego, CA, USA) was used to compute all statistical analyses.

3. Results

3.1. Characteristics of isolated EVs

To investigate EVs' role in cancer progression, first EVs were isolated and characterized from the conditioned media of all five syngeneic pairs of cell lines. Nanoparticle tracking analyses of the EV fractions confirmed the presence of EVs in the isolates. The isolated particles' mean size was 125–179 nm (Fig. 1A-B), which is consistent with the previously reported values for supernatant-derived EVs [52]. The particle concentration ranged from 8,3x109 to 35x109/ml. We compared the lipid concentration and EV-associated protein content of each cell line, however, no significant correlation with the cell lines' aggressivity was observed (Fig. 1C-D). Flow cytometry confirmed the presence of commonly used extracellular vesicle markers (EpCam, CD81, CD63, CD9, Annexin) [53]–[55] (Fig. 1E) with the least positivity for CD63.

3.2. Melanoma cell-derived EVs failed to impact cell viability

EVs' effect on cell viability was analyzed using SRB assay. To investigate the effect of EVs derived from more and less aggressive cell lines on cell viability, each EV-isolate (10 µg /ml protein content) was used to treat both members of the corresponding syngeneic pair of cell lines. Hence, each cell line was treated with vehicle (PBS), their own EVs, and their cell-pair's EVs (Fig. 2.). Mel Pt-1 post and WM983B cells treated with their own EVs showed a significant increase in cell viability, any other treatment with the more aggressive cell line-derived EV had only modest effect on cell viability. Similarly, treatments with the less-aggressive cells produced EVs had minimal effect on cell proliferation.

3.3. EV treatment failed to promote sphere growth

To investigate EVs' tumorigenic potential in the more complex 3D tumor model, spheroid growth assay was performed. All the investigated cell lines formed spheroids 24 hours after seeding, thus all could be treated with their own and their pairs' EVs. Photos from each spheroid by an inverse microscope were recorded daily for 7 days. As shown in Fig. 3. EV treatment resulted in only minor changes in spheroid growth. Effect of the treatment did not differ if cells were treated with EVs isolated from the supernatant originating from cells representing the more or less aggressive stage of the tumor.

3.4. Extracellular vesicles modify melanoma cells' migratory capacity

Video-microscopic measurements and subsequent single-cell tracking were performed to investigate a possible effect of EV treatment on cell motility (Fig. 4.). Two different commonly used parameters (MSD and TTD) were calculated to have a more detailed view of the changes in the migratory activity of the cells. Results are summarized in Fig. 5., MSD and TTD as a function of time is presented in Sup.Table 1.

A cell line-dependent effect of EV treatment on cell migration was observed. Mel Pt-1 pre/post, Mel Pt-3 post, WM983A, WM983B and M1 cells did not show significant differences in any of the calculated parameters if treated with EVs alone. Nevertheless, WM983A/WM983B EV treatment led to a modest increase in MSD and in TTD (Fig. 5. D). An increment in the migration of M1 cells was also observed following the treatment with A2058-derived-EVs (Fig. 5. E). In the case of the Mel Pt-3 pair of cell lines, the pre cells' migration was stimulated with both EVs, although a significant increase was only seen in MSD after the treatment with the post-cell-derived EVs (Fig. 5. B). Considering the Mel Pt-4 pre cell line only TTD appeared to be markedly increased (Fig. 5. C). Nonetheless, MSD of Mel Pt-4 post cells was significantly elevated if treated with pre-EV. Whereas increase in TTD failed to be significant. Interestingly, A2058 cell line's TTD was reduced as a reaction to EV treatment, however MSD was only decreased if the A2058 EVs were used for treatment. Altogether, there was no uniform difference between the migratory effect of less and more aggressive cell line-derived EVs.

3.5. EV treatment could compensate migration inhibitory effect of vemurafenib

After observing that EVs showed a more distinct effect on migration, we investigated that the BRAF inhibitor, vemurafenib, could undermine the effect of EVs in migration. First, we determined the vemurafenib sensitivity of the cell lines with SRB as-say (SupFig1.). A2058 – M1 and Mel Pt-1 pre – post cells' sensitivity did not differ. WM983A cells were more sensitive as compared to WM983B, its pair, deriving from the metastatic site. Similarly, Mel Pt-3 pre cells were more susceptible to vemurafenib as compared to the corresponding post cell line. In contrast, in Mel Pt-4, the observed vemurafenib sensitivity was higher in the post cells.

Vemurafenib concentrations around the cells' GI50 values were used for the vid-eo-microscopy experiments. The calculated ΔAUC values are shown in Fig. 4., MSD and TTD as a function of time is presented SupTable2. Vemurafenib markedly reduced cell migration quantified as MSD and TTD in most of the cell lines. Although, vemurafenib treatment did not show a migration inhibitory effect in TTD of WM983A, WM983B and Mel Pt-3 post cells. Of note, in Mel Pt-3 post cells MSD and TTD revealed opposite but not significant migratory effect.

In combination with EVs, vemurafenib could suppress the slight migration-promoting effect of EVs in Mel Pt-1 cells (Fig. 5. A). Similarly, in A2058 and M1 cells EVs could not significantly compensate for the migration inhibitory effect of vemurafenib, with the exception seen in TTD of A2058 cells if treated with vemurafenib in combination with M1-derived EVs (Fig. 5. E). In the more resistant cells (Mel Pt-3 post, Mel Pt-4 pre and WM983B) no significant difference in MSD and TTD was detected when treated with vemurafenib alone or in combination with EVs. In contrast, significantly higher MSD was measured in the more sensitive cells (Mel Pt-3 pre, Mel Pt-4 post and WM983A) after treatment with vemurafenib and EVs from the more resistant cells as compared to vemurafenib treatment. Interestingly, the same effect in TTD was significant only in WM983A cells.

4. Discussion

Extracellular vesicles are candidate key factors in the communication of normal and tumor cells [56]. Metastasis formation jeopardizes the life of cancer patients worldwide [19]. Thus, the involvement of EVs in cell migration and metastasis formation is highly investigated [8].

The present study investigated the potentially different effects of EVs produced by cells with different sensitivity to vemurafenib and modelling less and more advanced stage tumors. Five pairs of syngeneic melanoma cell lines were treated with EVs isolated from their or their pair's supernatant. Characterization of isolated EVs and determination of their effects on cell proliferation and migration were performed. Characteristics of the EVs isolated from the supernatant of the cells by ultracentrifugation were relatable with the previously described supernatant-derived EV fractions [14], [57]–[59].

Cancer cell migration, as an essential process of metastasis formation, is widely studied [60]. The effect of EV treatment on tumor cell migration is mostly investigated by transwell [10], [14], [17], [61]–[64] or wound healing assays [10], [64]–[68]. However, these assays are relatively complex and examine more aspects of the treatments' effects simultaneously, like proliferation and invasion, not only migration. Moreover, these complex assays investigate cells migratory capacity in one direction (e.g. the closing of the scratch or migration through the membrane), without considering the dynamic characteristics of cell migration [69], [70].

Single-cell tracking based methods, as used in this study, are more direct approaches to investigate the treatments' effect on cell migration. Two parameters MSD and TTD were calculated to quantify cell migration [50], [51]. In an earlier study, vid-eo-microscopy recording, and calculation of velocity could not prove migration-promoting effect of melanoma-derived EVs in cancer-associated fibroblasts [71].

In our results, for most of the cell lines, MSD and TTD values were elevated after EV treatments, although EVs from the more aggressive cell lines did not show an unequivocally greater effect. Since cell migration is crucial in metastasis formation, based on our results, we suggest, that EVs have a more prominent role in metastasis formation, rather than tumor growth. These results are in line with earlier findings that oral squamous carcinoma cells treated with cancer-associated fibroblasts derived EVs showed increased migration to a greater extent than proliferation [72]. Similarly, neither the non-tumorigenic and tumorigenic melanoma cell lines-derived EVs could affect the recipient cells' proliferation, however, EVs from the more tumorigenic cells could promote the recipient cells migration [17]. Possible reason why EVs promote migration could be that EVs could transfer integrins [73] and they can promote cell adhesion [74]. Moreover, EVs can affect the phosphorylation of FAK, AKT, and ERK1/2 [75] and transfer mRNAs [18] and miRNAs [76] involved in migration and metastasis formation. Proteome analysis of metastatic melanoma cell lines-derived EVs' by KEGG (Kyoto Encyclopedia of Genes and Genomes), BBID (Biological Biochemical Image Database), and Biocarta databases showed that EVs are enriched in proteins involved in the regulation of actin cytoskeleton and focal adhesion [17].

The selective BRAF V600E inhibitor, vemurafenib was widely used in clinics, however after the first promising period of the treatment, resistance occurred in many patients [39], that manifested in the acceleration of metastasis formation [43], [44]. Vemurafenib resistance can occur through multiple mechanisms, including EV-mediated intracellular cross-talks [59]. Our investigation revealed the migration-promoting role of EVs; therefore, we tested if these EV-related elevated metastatic potentials could be reversed by vemurafenib. However, in our experiments, we observed that the more vemurafenib-resistant cells-derived EVs could diminish the migration-inhibiting effect of vemurafenib. This is in line with the fact that EVs originating from V600E BRAF mutant PLX-4720-resistant cells could transmit resistance to the recipient cells by transporting PDGFRβ. In contrast, EVs from the sensitive parental cells were unable to promote proliferation [33]. Additionally, vemurafenib-resistant melanoma cells-derived EVs could increase the proliferation of sensitive cells during vemurafenib therapy compared to the control cells via transporting an ALK isoform [42]. Also, EVs from resistant cell lines and relapsed BRAFi-treated patient plasma are associated with BRAF splicing variants [77]. Moreover, plasma EV-associated miRNA analysis of MM patients revealed that their miRNA profile could predict the disease progression during MAPKi treatment [78]. Therefore, EVs from resistant cells could transfer specific features to the sensitive cells and help them overcome the BRAF inhibition [79].

5. Conclusions

In summary, melanoma-derived EVs did not modulate cancer cell proliferation profoundly, although their migration-promoting effect was remarkable. Moreover, EVs derived from the more resistant cell lines could compensate for the migration inhibitory effect of vemurafenib. Therefore, our findings are in line with several observations about EVs' role in melanoma progression, EVs have more prominent role in metastasis formation than primary tumor growth. Furthermore, their role in vemurafenib resistance has become more evident.

Declarations

Consent for publication: Not applicable.

Availability of data and materials: Not applicable.

Competing interests: Not applicable.

Funding: This research was supported by the National Research, Development and Innovation Office through the grant TKP2021-EGA-42.

Author Contributions: Conceptualization, A.N., Z.V., E.B. and T.G.; methodology, A.N., N.K.D., G.L.B., T.K., A.G. and D.K.; formal analysis, A.N., G.L.B., N.K.D., T.K. and A.G.; investigation, A.N., T.G., N.K.D, T.K., G.L.B., A.G.; resources and founding acquisition, M.D., I.T.; writ-ing—original draft preparation, A.N., G.L.B., T.K. and T.G.; writing—review and editing, A.M.Sz., N.K.D., Z.V., G.L.B. and T.G.; visualization, A.N., A.G., Z.V. and G.L.B. All authors have read and agreed to the published version of the manuscript.

Acknowledgments: Not applicable.

References

1. Czystowska-Kuzmicz M, Whiteside TL. “The potential role of tumor-derived exosomes in diagnosis, prognosis, and response to therapy in cancer,” Expert Opinion on Biological Therapy, vol. 21, no. 2. Taylor and Francis Ltd., pp. 241–258, 2021. doi: 10.1080/14712598.2020.1813276.
2. Zhu Q, et al. MiR-124-3p impedes the metastasis of non-small cell lung cancer via extracellular exosome transport and intracellular PI3K/AKT signaling. Biomark Res. Dec. 2023;11(1). 10.1186/s40364-022-00441-w.
3. Silva J et al. “Analysis of exosome release and its prognostic value in human colorectal cancer,” Genes Chromosomes Cancer, vol. 51, no. 4, pp. 409–418, Apr. 2012, doi: 10.1002/gcc.21926.
4. Ludwig S, et al. Suppression of lymphocyte functions by plasma exosomes correlates with disease activity in patients with head and neck cancer. Clin Cancer Res. Aug. 2017;23(16):4843–54. 10.1158/1078-0432.CCR-16-2819.
5. Peinado H et al. “Melanoma exosomes educate bone marrow progenitor cells toward a pro-metastatic phenotype through MET,” Nat Med, vol. 18, no. 6, pp. 883–891, Jun. 2012, doi: 10.1038/nm.2753.
6. Zorrilla SR, Pérez-Sayans M, Fais S, Logozzi M, Torreira MG, García AG. A pilot clinical study on the prognostic relevance of plasmatic exosomes levels in oral squamous cell carcinoma patients. Cancers (Basel). Mar. 2019;11(3). 10.3390/cancers11030429.
7. Carretero-González A, et al. Characterization of plasma circulating small extracellular vesicles in patients with metastatic solid tumors and newly diagnosed brain metastasis. Oncoimmunology. 2022;11(1). 10.1080/2162402X.2022.2067944.

8. Seibold T, Waldenmaier M, Seufferlein T, Eiseler T. Small extracellular vesicles and metastasis—blame the messenger. Cancers (Basel). Sep. 2021;13(17). 10.3390/cancers13174380.
9. Urabe F, Patil K, Ramm GA, Ochiya T, Soekmadji C. “Extracellular vesicles in the development of organ-specific metastasis,” Journal of Extracellular Vesicles, vol. 10, no. 9. John Wiley and Sons Inc, Jul. 01, 2021. doi: 10.1002/jev2.12125.
10. Mazurkiewicz J, et al. Melanoma cells with diverse invasive potential differentially induce the activation of normal human fibroblasts. Cell Communication and Signaling. Dec. 2022;20(1). 10.1186/s12964-022-00871-x.
11. Popěna I, et al. Effect of colorectal cancer-derived extracellular vesicles on the immunophenotype and cytokine secretion profile of monocytes and macrophages. Cell Communication and Signaling. Apr. 2018;16(1). 10.1186/s12964-018-0229-y.
12. Matsumoto A et al. “Accelerated growth of B16BL6 tumor in mice through efficient uptake of their own exosomes by B16BL6 cells,” Cancer Sci, vol. 108, no. 9, pp. 1803–1810, Sep. 2017, doi: 10.1111/cas.13310.
13. Sung BH, Parent CA, Weaver AM. “Extracellular vesicles: Critical players during cell migration,” Developmental Cell, vol. 56, no. 13. Cell Press, pp. 1861–1874, Jul. 12, 2021. doi: 10.1016/j.devcel.2021.03.020.
14. Mannavola F, Tucci M, Felici C, Passarelli A, D’Oronzo S, Silvestris F. “Tumor-derived exosomes promote the in vitro osteotropism of melanoma cells by activating the SDF-1/CXCR4/CXCR7 axis,” J Transl Med, vol. 17, no. 1, Jul. 2019, doi: 10.1186/s12967-019-1982-4.
15. Isola AL, Eddy K, Zembrzuski K, Goydos JS, Chen S. “Exosomes released by metabotropic glutamate receptor 1 (GRM1) expressing melanoma cells increase cell migration and invasiveness,” 2017. [Online]. Available: www.impactjournals.com/oncotarget.
16. Peinado H et al. “Pre-metastatic niches: Organ-specific homes for metastases,” Nature Reviews Cancer, vol. 17, no. 5. Nature Publishing Group, pp. 302–317, May 01, 2017. doi: 10.1038/nrc.2017.6.
17. Lazar I et al. “Proteome characterization of melanoma exosomes reveals a specific signature for metastatic cell lines,” Pigment Cell Melanoma Res, vol. 28, no. 4, pp. 464–475, Jul. 2015, doi: 10.1111/pcmr.12380.
18. Zomer A, et al. In vivo imaging reveals extracellular vesicle-mediated phenocopying of metastatic behavior. Cell. May 2015;161(5):1046–57. 10.1016/j.cell.2015.04.042.
19. Bergers G, Fendt SM. “The metabolism of cancer cells during metastasis,” Nature Reviews Cancer, vol. 21, no. 3. Nature Research, pp. 162–180, Mar. 01, 2021. doi: 10.1038/s41568-020-00320-2.
20. Pagliuca C, Di Leo L, De Zio D. “New Insights into the Phenotype Switching of Melanoma,” Cancers, vol. 14, no. 24. MDPI, Dec. 01, 2022. doi: 10.3390/cancers14246118.
21. Turner N, Ware O, Bosenberg M. Genetics of metastasis: melanoma and other cancers. Clin Exp Metastasis. Aug. 2018;35:5–6. 10.1007/s10585-018-9893-y.
22. Hossain SM, Eccles MR. Phenotype Switching and the Melanoma Microenvironment; Impact on Immunotherapy and Drug Resistance. Int J Mol Sci. Jan. 2023;24(2):1601. 10.3390/ijms24021601.

23. Halle BR, Johnson DB. “Defining and Targeting BRAF Mutations in Solid Tumors,” Current Treatment Options in Oncology, vol. 22, no. 4. Springer, Apr. 01, 2021. doi: 10.1007/s11864-021-00827-2.
24. Savoia P, Fava P, Casoni F, Cremona O. Targeting the ERK signaling pathway in melanoma. Int J Mol Sci. 2019;20. 10.3390/ijms20061483. no. 6. MDPI AG, Mar.
25. Davies H et al. “Mutations of the BRAF gene in human cancer,” 2002. [Online]. Available: www.nature.com/nature.
26. McArthur GA, et al. Safety and efficacy of vemurafenib in BRAFV600E and BRAFV600K mutation-positive melanoma (BRIM-3): Extended follow-up of a phase 3, randomised, open-label study. Lancet Oncol. 2014;15(3):323–32. 10.1016/S1470-2045(14)70012-9.
27. Chapman PB et al. “Vemurafenib in patients with BRAFV600 mutation-positive metastatic melanoma: Final overall survival results of the randomized BRIM-3 study,” Annals of Oncology, vol. 28, no. 10, pp. 2581–2587, Oct. 2017, doi: 10.1093/annonc/mdx339.
28. McArthur GA et al. “Vemurafenib in metastatic melanoma patients with brain metastases: An open-label, single-arm, phase 2, multicentre study,” Annals of Oncology, vol. 28, no. 3, pp. 634–641, Mar. 2017, doi: 10.1093/annonc/mdw641.
29. Sosman JA, et al. Survival in BRAF V600–Mutant Advanced Melanoma Treated with Vemurafenib. N Engl J Med. Feb. 2012;366:707–14. 10.1056/NEJMoa1112302.
30. Weitzenböck HP et al. “Proteome analysis of NRF2 inhibition in melanoma reveals CD44 up-regulation and increased apoptosis resistance upon vemurafenib treatment,” Cancer Med, vol. 11, no. 4, pp. 956–967, Feb. 2022, doi: 10.1002/cam4.4506.
31. Tang F, Li S, Liu D, Chen J, Han C. Sorafenib sensitizes melanoma cells to vemurafenib through ferroptosis. Transl Cancer Res. 2020;9(3):1584–93. 10.21037/tcr.2020.01.62.
32. Liu W et al. “KSRP modulates melanoma growth and efficacy of vemurafenib,” Biochim Biophys Acta Gene Regul Mech, vol. 1862, no. 8, pp. 759–770, Aug. 2019, doi: 10.1016/j.bbagrm.2019.06.005.
33. Hartman ML, Rozanski M, Osrodek M, Zalesna I, Czyz M. “Vemurafenib and trametinib reduce expression of CTGF and IL-8 in V600EBRAF melanoma cells,” Laboratory Investigation, vol. 97, no. 2, pp. 217–227, Feb. 2017, doi: 10.1038/labinvest.2016.140.
34. Barceló C et al. “T-Type Calcium Channels as Potential Therapeutic Targets in Vemurafenib-Resistant BRAFV600E Melanoma,” Journal of Investigative Dermatology, vol. 140, no. 6, pp. 1253–1265, Jun. 2020, doi: 10.1016/j.jid.2019.11.014.
35. Radić M, et al. Characterization of Vemurafenib-Resistant Melanoma Cell Lines Reveals Novel Hallmarks of Targeted Therapy Resistance. Int J Mol Sci. Sep. 2022;23(17). 10.3390/ijms23179910.
36. Kim N et al. “Novel and potent small molecules against melanoma harboring braf class i/ii/iii mutants for overcoming drug resistance,” Int J Mol Sci, vol. 22, no. 7, Apr. 2021, doi: 10.3390/ijms22073783.
37. Vella LJ, Behren A, Coleman B, Greening DW, Hill AF, Cebon J. “Intercellular Resistance to BRAF Inhibition Can Be Mediated by Extracellular Vesicle–Associated PDGFRβ,” Neoplasia (United States), vol. 19, no. 11, pp. 932–940, Nov. 2017, doi: 10.1016/j.neo.2017.07.002.

38. Lunavat TR, et al. BRAFV600 inhibition alters the microRNA cargo in the vesicular secretome of malignant melanoma cells. Proc Natl Acad Sci U S A. Jul. 2017;114(29):E5930–9. 10.1073/pnas.1705206114.
39. Skudalski L, Waldman R, Kerr PE, Grant-Kels JM. “Melanoma: An update on systemic therapies,” Journal of the American Academy of Dermatology, vol. 86, no. 3. Elsevier Inc., pp. 515–524, Mar. 01, 2022. doi: 10.1016/j.jaad.2021.09.075.
40. Rossi A, Roberto M, Panebianco M, Botticelli A, Mazzuca F, Marchetti P. “Drug resistance of BRAF-mutant melanoma: Review of up-to-date mechanisms of action and promising targeted agents,” European Journal of Pharmacology, vol. 862. Elsevier B.V., Nov. 05, 2019. doi: 10.1016/j.ejphar.2019.172621.
41. Atzori MG, et al. Role of VEGFR-1 in melanoma acquired resistance to the BRAF inhibitor vemurafenib. J Cell Mol Med. Jan. 2020;24(1):465–75. 10.1111/jcmm.14755.
42. Cesi G, et al. A new ALK isoform transported by extracellular vesicles confers drug resistance to melanoma cells. Mol Cancer. Oct. 2018;17(1). 10.1186/s12943-018-0886-x.
43. Imafuku K, Yoshino K, Yamaguchi K, Tsuboi S, Ohara K, Hata H. “Sudden Onset of Brain Metastasis despite the Use of Vemurafenib for Another Metastatic Lesion in Malignant Melanoma Patients,” Case Rep Oncol, vol. 10, no. 1, pp. 290–295, Jan. 2017, doi: 10.1159/000461576.
44. Puzanov I, et al. Long-term outcome in BRAFV600E melanoma patients treated with vemurafenib: Patterns of disease progression and clinical management of limited progression. Eur J Cancer. 2015;51(11):1435–43. 10.1016/j.ejca.2015.04.010.
45. Lai F, Jiang CC, Farrelly ML, Zhang XD, Hersey P. “Evidence for upregulation of Bim and the splicing factor SRp55 in melanoma cells from patients treated with selective BRAF inhibitors,” Melanoma Res, vol. 22, no. 3, pp. 244–251, Jun. 2012, doi: 10.1097/CMR.0b013e328353eff2.
46. Timár J, Kovalszky I, Paku S, Lapis K, Kopper L. “Two human melanoma xenografls with different metastatic capacity and glycosaminoglycan pattern,” 1989.
47. Théry C, et al. Minimal information for studies of extracellular vesicles 2018 (MISEV2018): a position statement of the International Society for Extracellular Vesicles and update of the MISEV2014 guidelines. J Extracell Vesicles. Jan. 2018;7(1). 10.1080/20013078.2018.1535750.
48. Visnovitz T, et al. An improved 96 well plate format lipid quantification assay for standardisation of experiments with extracellular vesicles. J Extracell Vesicles. Jan. 2019;8(1). 10.1080/20013078.2019.1565263.
49. Van Deun J, et al. EV-TRACK: Transparent reporting and centralizing knowledge in extracellular vesicle research. Nat Methods. 2017;14(28):228–32. 10.1038/nmeth.4185. no. 3Nature Publishing Group.
50. Piccinini F, Kiss A, Horvath P. CellTracker (not only) for dummies. Bioinformatics. Mar. 2016;32(6):955–7. 10.1093/bioinformatics/btv686.
51. Masuzzo P, Van Troys M, Ampe C, Martens L. “Taking Aim at Moving Targets in Computational Cell Migration,” Trends in Cell Biology, vol. 26, no. 2. Elsevier Ltd, pp. 88–110, Feb. 01, 2016. doi:

10.1016/j.tcb.2015.09.003.

52. Allelein S, et al. Potential and challenges of specifically isolating extracellular vesicles from heterogeneous populations. Sci Rep. Dec. 2021;11(1). 10.1038/s41598-021-91129-y.
53. Lattmann E, Levesque MP. “The Role of Extracellular Vesicles in Melanoma Progression,” Cancers, vol. 14, no. 13. MDPI, Jul. 01, 2022. doi: 10.3390/cancers14133086.
54. Larson MC, Woodliff JE, Hillery CA, Kearl TJ, Zhao M. “Phosphatidylethanolamine is externalized at the surface of microparticles,” Biochim Biophys Acta Mol Cell Biol Lipids, vol. 1821, no. 12, pp. 1501–1507, Dec. 2012, doi: 10.1016/j.bbalip.2012.08.017.
55. Ekström K, Crescitelli R, Pétursson HI, Johansson J, Lässer C, Bagge RO. Characterization of surface markers on extracellular vesicles isolated from lymphatic exudate from patients with breast cancer. BMC Cancer. Dec. 2022;22(1). 10.1186/s12885-021-08870-w.
56. Yáñez-Mó M et al. “Biological properties of extracellular vesicles and their physiological functions,” Journal of Extracellular Vesicles, vol. 4, no. 2015. Co-Action Publishing, pp. 1–60, 2015. doi: 10.3402/jev.v4.27066.
57. Ciftci E, Bozbeyoglu N, Gursel I, Korkusuz F, Misirlioglu FB, Korkusuz P. “Comparative analysis of magnetically activated cell sorting and ultracentrifugation methods for exosome isolation,” PLoS One, vol. 18, no. 2 February, Feb. 2023, doi: 10.1371/journal.pone.0282238.
58. Jeppesen DK, et al. Comparative analysis of discrete exosome fractions obtained by differential centrifugation. J Extracell Vesicles. 2014;3(1). 10.3402/jev.v3.25011.
59. Gener Lahav T et al. “Melanoma-derived extracellular vesicles instigate proinflammatory signaling in the metastatic microenvironment,” Int J Cancer, vol. 145, no. 9, pp. 2521–2534, Nov. 2019, doi: 10.1002/ijc.32521.
60. Majidpoor J, Mortezaee K. “Steps in metastasis: an updated review,” Medical Oncology, vol. 38, no. 1. Springer, Jan. 01, 2021. doi: 10.1007/s12032-020-01447-w.
61. Sakha S, Muramatsu T, Ueda K, Inazawa J. “Exosomal microRNA miR-1246 induces cell motility and invasion through the regulation of DENND2D in oral squamous cell carcinoma,” Sci Rep, vol. 6, Dec. 2016, doi: 10.1038/srep38750.
62. Sun LP, et al. Cancer-associated fibroblast-derived exosomal miR-382-5p promotes the migration and invasion of oral squamous cell carcinoma. Oncol Rep. 2019;42(4):1319–28. 10.3892/or.2019.7255.
63. Gu H, et al. Exosomes derived from human mesenchymal stem cells promote gastric cancer cell growth and migration via the activation of the Akt pathway. Mol Med Rep. Oct. 2016;14(4):3452–8. 10.3892/mmr.2016.5625.
64. Clerici SP, Peppelenbosch M, Fuhler G, Consonni SR, Ferreira-Halder CV. “Colorectal Cancer Cell-Derived Small Extracellular Vesicles Educate Human Fibroblasts to Stimulate Migratory Capacity,” Front Cell Dev Biol, vol. 9, Jul. 2021, doi: 10.3389/fcell.2021.696373.
65. Wang X et al. “Fetal dermal mesenchymal stem cell-derived exosomes accelerate cutaneous wound healing by activating Notch signaling,” Stem Cells Int, vol. 2019, 2019, doi: 10.1155/2019/2402916.

66. Bychkov ML, et al. Extracellular Vesicles Derived from Acidified Metastatic Melanoma Cells Stimulate Growth, Migration, and Stemness of Normal Keratinocytes. Biomedicines. Mar. 2022;10(3). 10.3390/biomedicines10030660.
67. Yang B, “High-metastatic cancer cells derived exosomal miR92a-3p promotes epithelial-mesenchymal transition and metastasis of low-metastatic cancer cells by regulating PTEN/Akt pathway in hepatocellular carcinoma,”, Oncogene et al. vol. 39, no. 42, pp. 6529–6543, Oct. 2020, doi: 10.1038/s41388-020-01450-5.
68. Endzeliņs E et al. “Extracellular vesicles derived from hypoxic colorectal cancer cells confer metastatic phenotype to non-metastatic cancer cells,” Anticancer Res, vol. 38, no. 9, pp. 5139–5147, Sep. 2018, doi: 10.21873/anticanres.12836.
69. Pijuan J et al. “In vitro cell migration, invasion, and adhesion assays: From cell imaging to data analysis,” Front Cell Dev Biol, vol. 7, no. JUN, 2019, doi: 10.3389/fcell.2019.00107.
70. Gau D, Roy P. Single Cell Migration Assay Using Human Breast Cancer MDA-MB-231 Cell Line. Bio Protoc. 2020;10(8). 10.21769/bioprotoc.3586.
71. Strnadová K, et al. Exosomes produced by melanoma cells significantly influence the biological properties of normal and cancer-associated fibroblasts. Histochem Cell Biol. Feb. 2022;157(2):153–72. 10.1007/s00418-021-02052-2.
72. Dourado MR, et al. Extracellular vesicles derived from cancer-associated fibroblasts induce the migration and invasion of oral squamous cell carcinoma. J Extracell Vesicles. Jan. 2019;8(1). 10.1080/20013078.2019.1578525.
73. Singh A, Fedele C, Lu H, Nevalainen MT, Keen JH, Languino LR. “Exosome-mediated transfer of αvβ3 integrin from tumorigenic to nontumorigenic cells promotes a migratory phenotype,” Molecular Cancer Research, vol. 14, no. 11, pp. 1136–1146, Nov. 2016, doi: 10.1158/1541-7786.MCR-16-0058.
74. Sung BH, Ketova T, Hoshino D, Zijlstra A, Weaver AM. Directional cell movement through tissues is controlled by exosome secretion. Nat Commun. May 2015;6. 10.1038/ncomms8164.
75. JANPIPATKUL K, PANVONGSA W, WORAKITCHANON W, REUNGWETWATTANA T, CHAIROUNGDUA A. Extracellular Vesicles from EGFR T790M/L858R-mutant Non-small Cell Lung Cancer Promote Cancer Progression. Anticancer Res. 2022;42(8):3835–44. 10.21873/anticanres.15874.
76. Luan W, et al. Exosomal miR-106b-5p derived from melanoma cell promotes primary melanocytes epithelial-mesenchymal transition through targeting EphA4. J Experimental Clin Cancer Res. Dec. 2021;40(1). 10.1186/s13046-021-01906-w.
77. Clark ME et al. “Detection of BRAF splicing variants in plasma-derived cell-free nucleic acids and extracellular vesicles of melanoma patients failing targeted therapy therapies,” 2020. [Online]. Available: www.oncotarget.com.
78. Svedman FC, et al. Extracellular microvesicle microRNAs as predictive biomarkers for targeted therapy in metastastic cutaneous malignant melanoma. PLoS ONE. Nov. 2018;13(11). 10.1371/journal.pone.0206942.

79. Kluszczynska K, Czyz M. “Extracellular Vesicles-Based Cell-Cell Communication in Melanoma: New Perspectives in Diagnostics and Therapy,” International Journal of Molecular Sciences, vol. 24, no. 2. MDPI, Jan. 01, 2023. doi: 10.3390/ijms24020965.

Figures

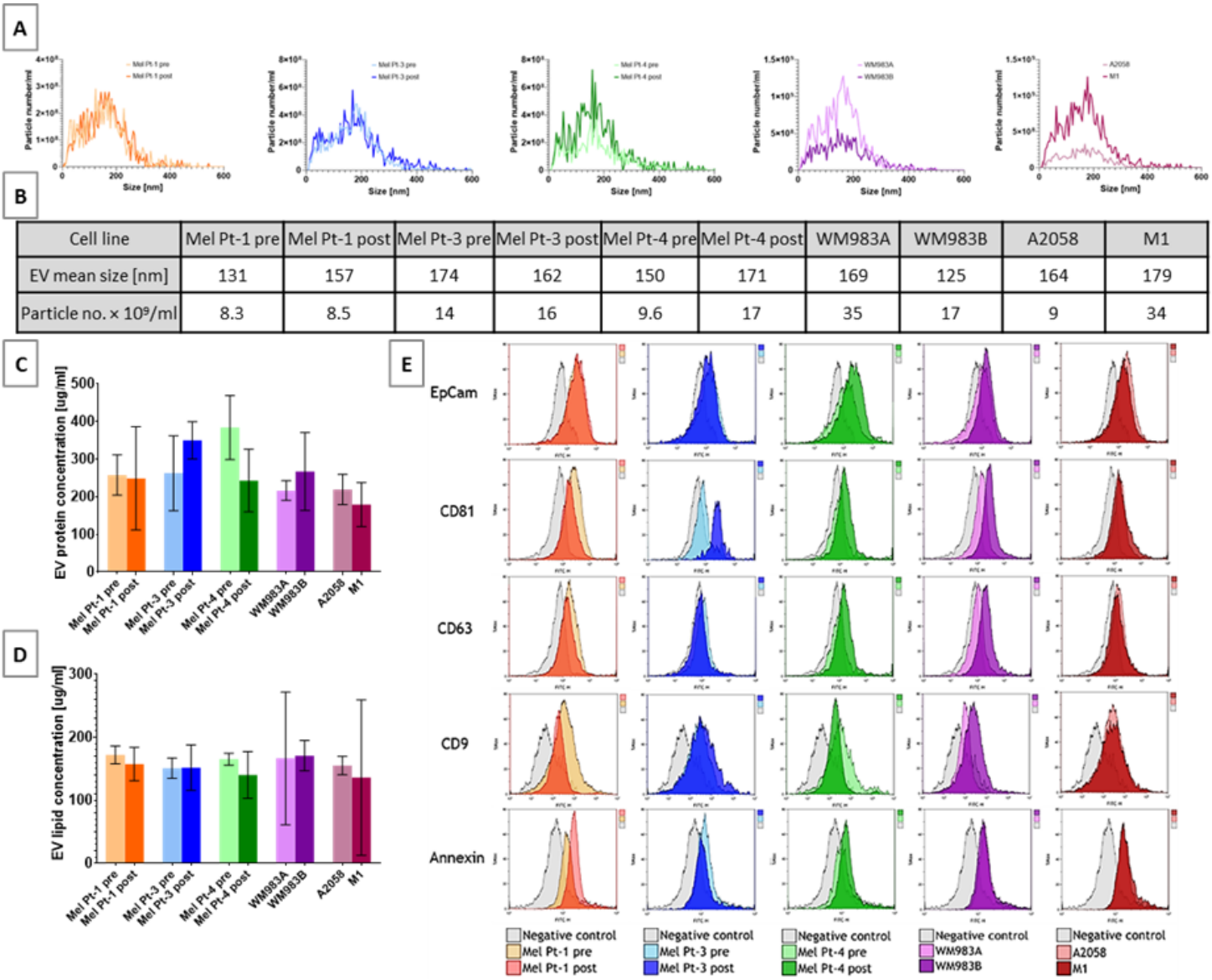

Cell line	Mel Pt-1 pre	Mel Pt-1 post	Mel Pt-3 pre	Mel Pt-3 post	Mel Pt-4 pre	Mel Pt-4 post	WM983A	WM983B	A2058	M1
EV mean size [nm]	131	157	174	162	150	171	169	125	164	179
Particle no. × 10⁹/ml	8.3	8.5	14	16	9.6	17	35	17	9	34

Figure 1

Characteristics of isolated extracellular vesicles. A) Concentration and size distribution measured by Nanoparticle Tracking Analysis; B) Mean size and particle number ×10^9/ml isolate (SD≤10%); C) EV sample protein concentration (µg/ml; mean ± 95% CI); D) EV fraction lipid concentration (µg/ml; mean ± 95% CI); E) Flow cytometry analysis of EV markers with their isotype control latex-beads

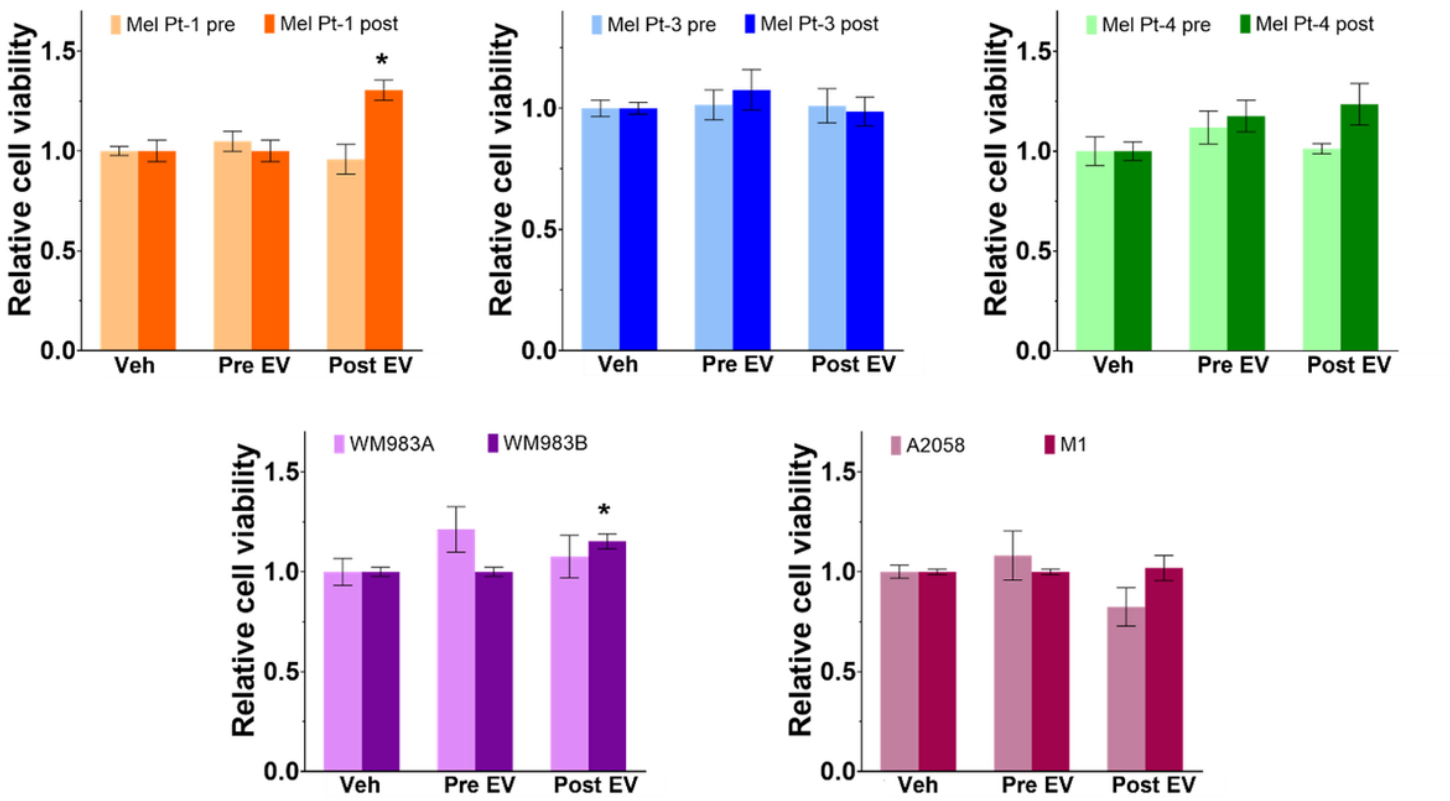

Figure 2

Extracellular vesicle's effect on cell viability measured by SRB assay. Cells were treated with their own and pair-derived EV isolate (10 µg/ml protein content) for 72 hours. Asterisks indicate significant difference to control using Kruskal-Wallis and Dunn's multiple comparison test. Results of three independent measurements are shown as mean ± SEM, and p-value less than 0.05 considered as statistically significant.

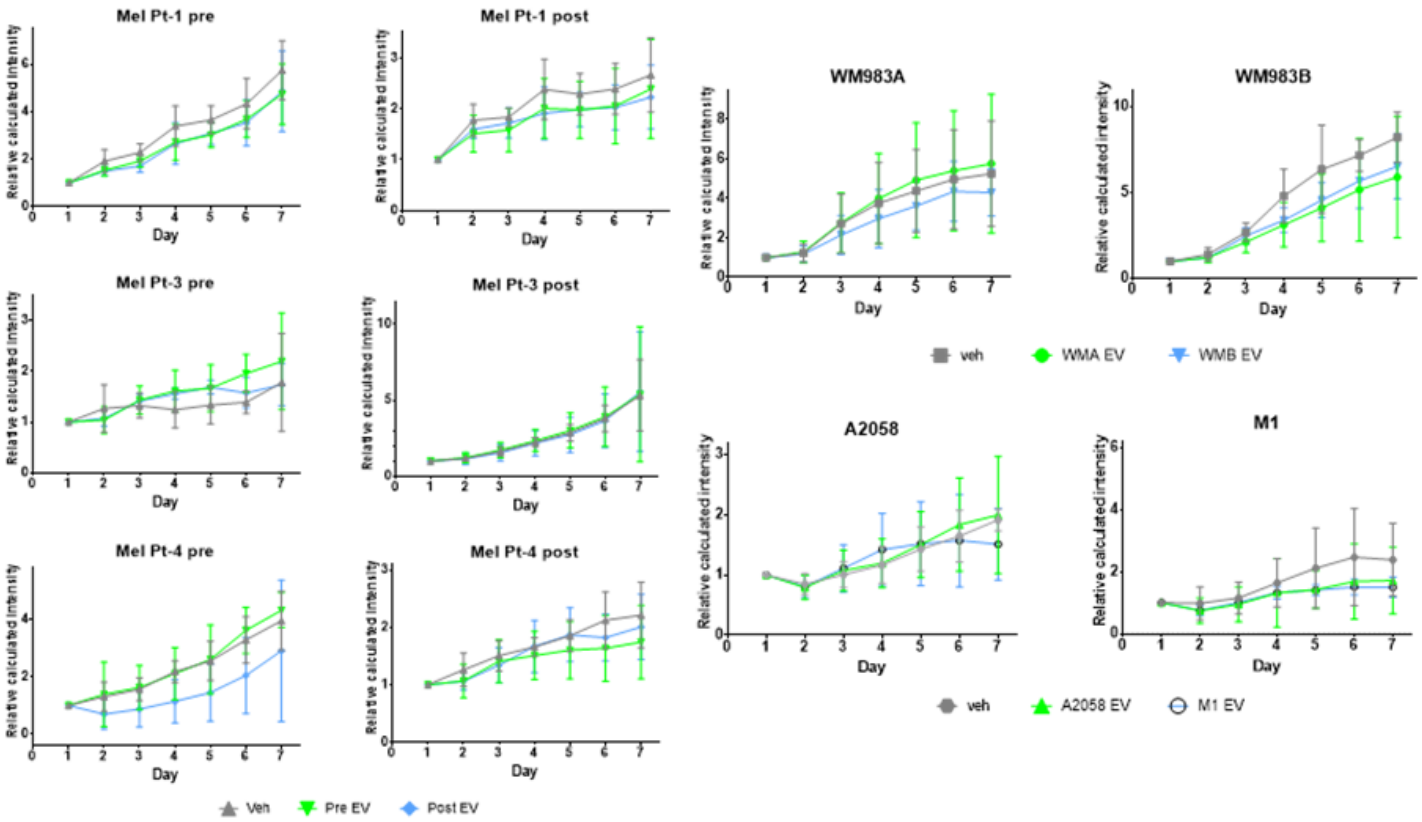

Figure 3

Effect of EV treatment on sphere growth. Cells were treated with their own and pair-derived EV fractions (10 µg/ml protein content) and spheroid formation was monitored for 7 days. Spheroid size was calculated based on diameter, area, integrated density and median pixel intensity of the respective well and spheroids. Calculated intensity is shown relative to the first day as mean ± 95% CI (n=6)

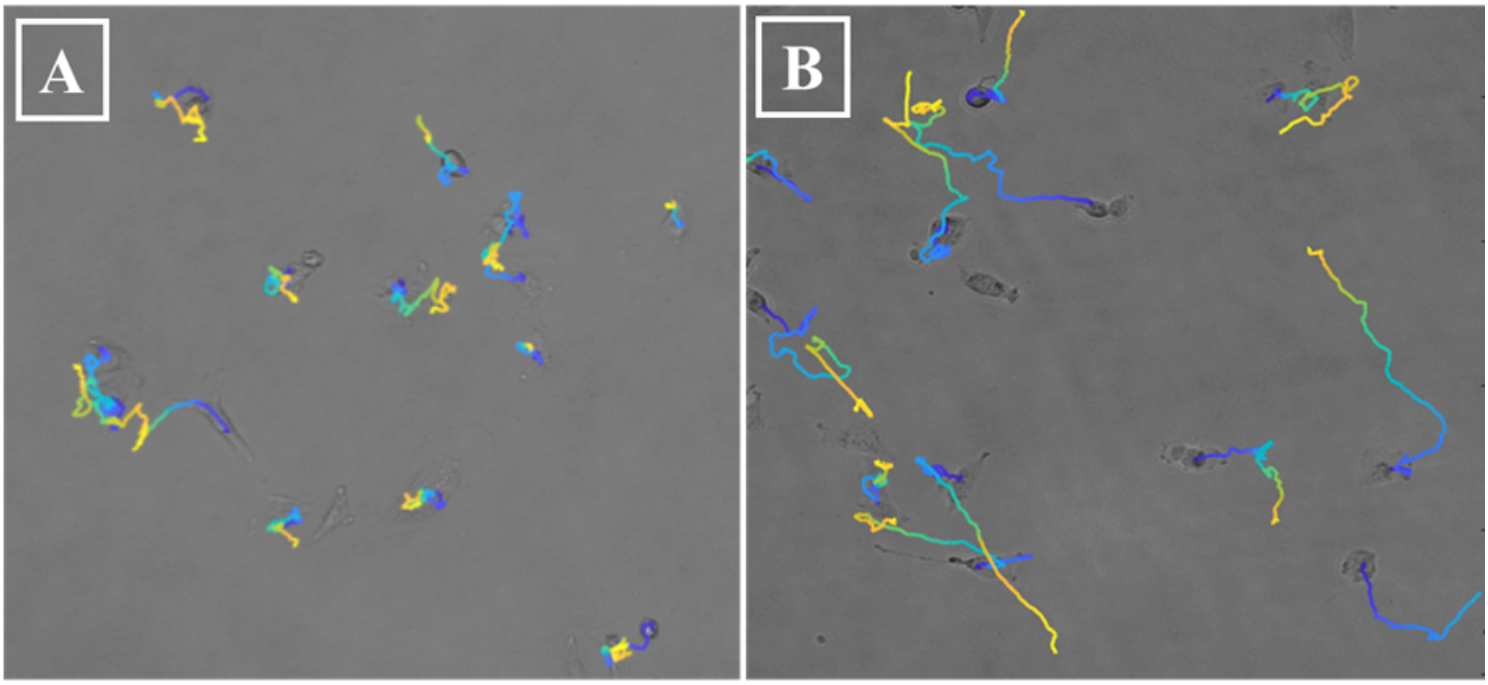

Figure 4

Trajectories of individual cells, drawn by marking the position of the cells and connecting these points during the whole recording. The color of the depicted trajectories refers to the time elapsed in the order of blue-green-yellow. A) Vehicle control; B) EV treated Mel Pt-4 post cells.

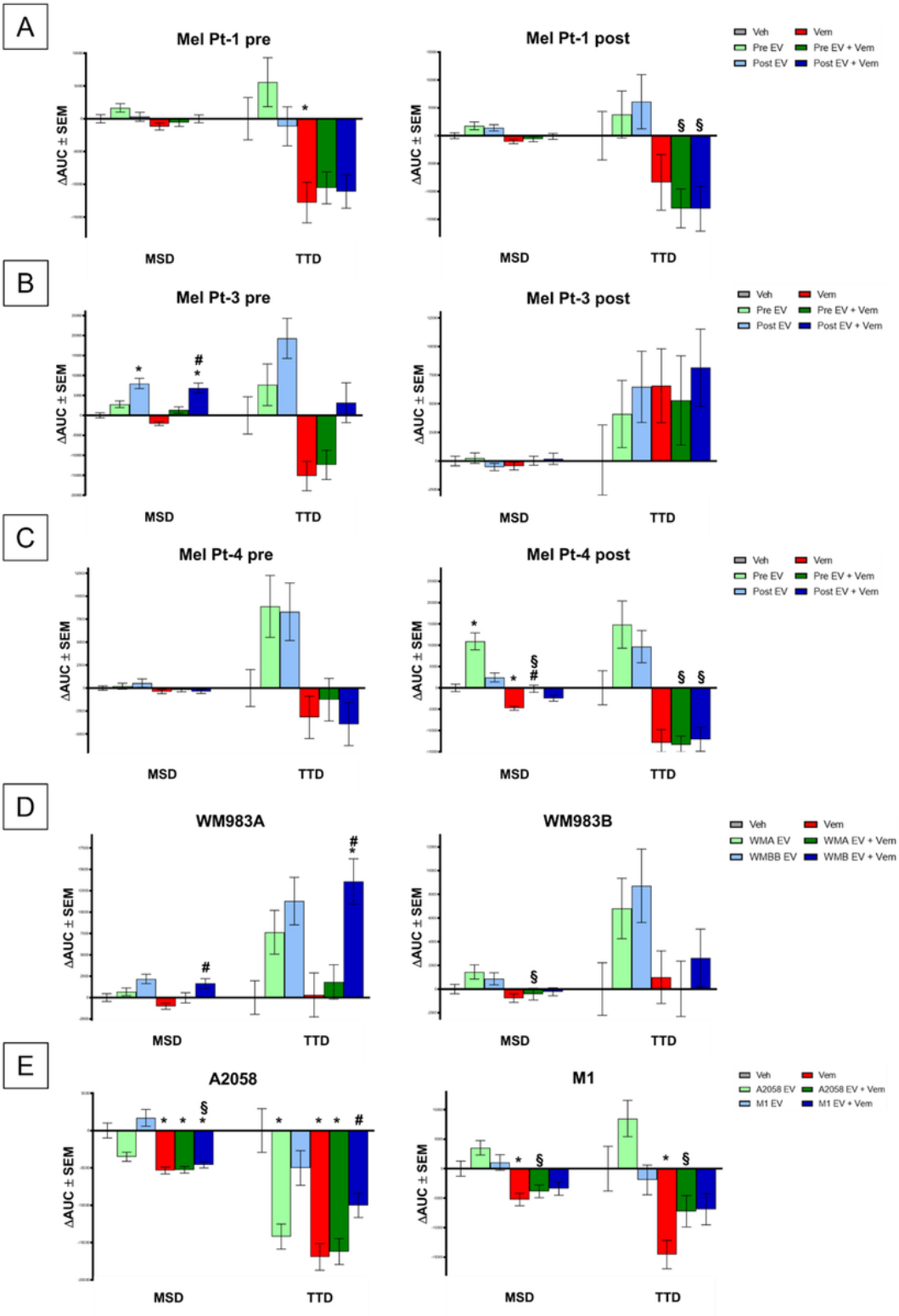

Figure 5

Effect of EV, vemurafenib (Vem) and combined treatment on single-cell migration. Cell migration was recorded for 24 hours, semiautomatic tracking of single cells performed using CellTracker and MSD and TTD calculated. Results of three independent measurements are shown as mean ± SEM, and p-value less than 0.05 considered as statistically significant. (to vehicle: *, to Vem: #, to EV-only: ¤)

Supplementary Files

This is a list of supplementary files associated with this preprint. Click to download.

- Nmethetal.Extracellularvesiclespromotemigration...Supplement1.zip